

Improved Polarization-Reconfigurable U-Slotted Patch Antennas Using MEMS Technologies

[#]Kazushi Nishizawa ¹, Kyosuke Mochizuki ¹, Hiromoto Inoue ², Yukihiisa Yoshida ², Yasuhiko Urata ³, Hiroaki Miyashita ¹, and Shigeru Makino ¹

¹Information Technology R&D Center, Mitsubishi Electric Corporation,
5-1-1 Ofuna, Kamakura-shi, Kanagawa 247-8501, Japan,
E-mail: Nishizawa.Kazushi@dp.MitsubishiElectric.co.jp

²Advanced Technology R&D Center, Mitsubishi Electric Corporation

³Kamakura Works, Mitsubishi Electric Corporation

1. Introduction

In recent years, reconfigurable antennas have been studied by several research organizations since their high performance (the ability to change the range of frequency, the direction of radiation, and so on) is extremely attractive and useful for many applications [1], [2]. As switching elements, semiconductor switches, that is, a PIN (p-intrinsic-n) diode or an FET (field effect transistor) and an RF-MEMS switch are assumed to be integrated with the antenna. The latter switch has the advantages of miniaturization, lower power consumption, and much lower transmission losses when the MEMS process is used. In addition, by using the MEMS process, switches that are integrated on the body of an antenna can be easily manufactured. Based on these advantages, MEMS-based reconfigurable antennas are found to be excellent for facilitating mass production and providing low costs.

In a previous study, we proposed a polarization-reconfigurable U-slotted patch antenna that can switch between two orthogonal polarizations by means of cantilever switches loaded on portions of a slotted patch antenna [3]. In addition, the feasibility and effectiveness of this antenna were verified by the results of a simulation and experiment. This study aims to realize a reconfigurable antenna with a higher performance, particularly with respect to the characteristic of electric power resistance, for which the improvement in the proposed antenna structure is studied by simulations. First, the geometry and basic operation of the antenna are presented. Next, the current distribution on the antenna surface is analyzed by a simulator. The result of this analysis is compared with that of the test for the electric power resistance conducted using the prototype. Finally, an improved structure that can withstand a large input electric power is developed.

2. MEMS-Switched U-Slotted Patch Antenna for Dual Polarization

The geometry of the polarization-reconfigurable antenna is shown in Fig. 1. A square, loop-shaped slot line that divides the patch conductor into interior and exterior sections is located at the centre of the square patch antenna. Cantilever-type MEMS switches are mounted at two opposite vertexes of the square loop. It is noted that the patch antenna and the switches are integrated easily by using the MEMS process. One of the remaining two vertexes is short-circuited with a conductor line of small length connected between the interior and exterior conductors and the other vertex is open-circuited. Input power is fed through feed pins situated on the backside of the centre of the internal conductor. When one of the MEMS switches is in the ON state and the other is in the OFF state, a U-slotted patch antenna is formed with a linear polarization. Thus, by changing the state of each switch, the antenna can switch between two orthogonal polarizations without undergoing mechanical movement; this is a remarkable characteristic of the antenna.

For example, when Switch 1 (SW#1) is ON and Switch 2 (SW#2) is OFF, the U-slot can be considered to be open along the y-axis, as shown in Fig. 2 (a); polarization is radiated along the

y-axis during this time. Conversely, when SW#1 is OFF and SW#2 is ON, the U-slot is formed sideways and polarization is radiated along the x-axis, as shown in Fig. 2 (b). In these cases, undesired resonance does not occur at the operating frequency because the length of the short-circuit slot between the terminals on the open side of the U-slot is shorter than the wavelength. Furthermore, when both switches are either ON or OFF, the U-slot cannot be formed; consequently, the antenna does not function at the desired frequency.

For controlling the switches, bias lines are wired on the co-surface of the antenna by using an air bridge structure and a gap in the patch conductor, as shown in Fig. 1.

3. Current Distribution on the Antenna Surface

An antenna loaded with MEMS switches is developed on a high-resistance Si wafer that is suited to the MEMS process. The thickness of the Si wafer is 0.018 wavelength (relative permittivity = 11.9) [3]. The prototype model is shown in Fig. 2.

The observation points of the current distribution on the antenna surface are shown as sections #1 to #5 in Fig. 1. Table 1 shows the simulated value of the current density at each section when SW#1 is ON and SW#2 is OFF. In addition, the current distribution at section #1 is shown in Fig. 3 (a). It is confirmed that the current density of section #1, which is a conductor of narrow width located under the air bridge, is higher than the current densities of the other sections. Since the bias line crosses over this section, the width of the conductor is very small with respect to the surroundings. In addition, because the switches and the bias lines are integrated with the patch conductor by using MEMS technologies, the thickness of the conductor at this section is small with respect to the surroundings. These are the major factors that contribute to the high current density.

4. Characteristic of Electric Power Resistance

In order for the antenna shown in Fig. 1 to exhibit a high electric power resistance, it is necessary to remove the portion where the current density is extremely high, such as section #1. In the MEMS process, because a change in the thickness of the conductor affects the entire antenna design, the thickness of the conductor is generally not changed. Hence, the conductor width is expanded within the possible range at which the air bridge structure can be manufactured by the MEMS process. In the experiment, for a large input electric power using the prototype, it is observed that section #1 breaks the earliest.

Fig. 3 (b) shows the current distribution at section #1 when the width is twice the original width shown in Fig. 1. The current density decreases to the same level as the current densities of the other sections, and it is shown that the characteristic of the electric power resistance of the antenna is improved. It is noted that the modification does not cause degradation in the antenna characteristics.

5. Conclusion

The improved structure of the polarization-reconfigurable U-slotted patch antenna with MEMS switches for handling the electric power resistance was presented based on the simulation and experimental results.

References

- [1] S. Onat, L. Alatan, and S. Demir, "Design of Triple-Band Reconfigurable Microstrip Antenna Employing RF-MEMS Switches," *Proc. in 2004 IEEE Antennas and Propagation Society International Symposium*, Monterey, July 2004.

- [2] L. Petit, L. Dussopt, and J. Laheurte, "MEMS-Switched Parasitic-Antenna Array for Radiation Pattern Diversity," *IEEE Trans. Antennas Propagat.*, vol. 54, no. 9, pp. 2624–2631, Sept. 2006.
- [3] K. Mochizuki, K. Nishizawa, H. Inoue, Y. Urata, Y. Yoshida, H. Miyashita, and S. Makino, "RF-MEMS Reconfigurable U-Slotted Patch Antennas for Dual Polarization," *Proc. in 2006 International Symposium on Antennas and Propagation*, Singapore, Nov. 2006.

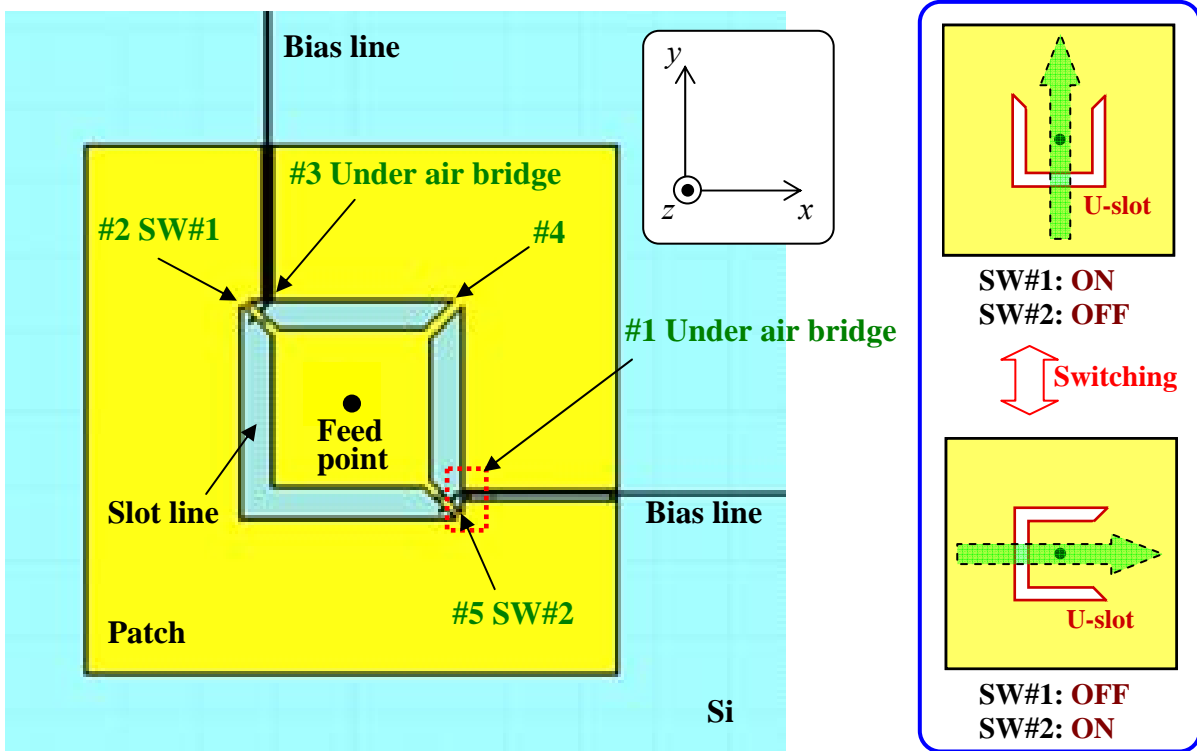


Fig. 1: Geometry of the MEMS-switched U-slotted patch antenna

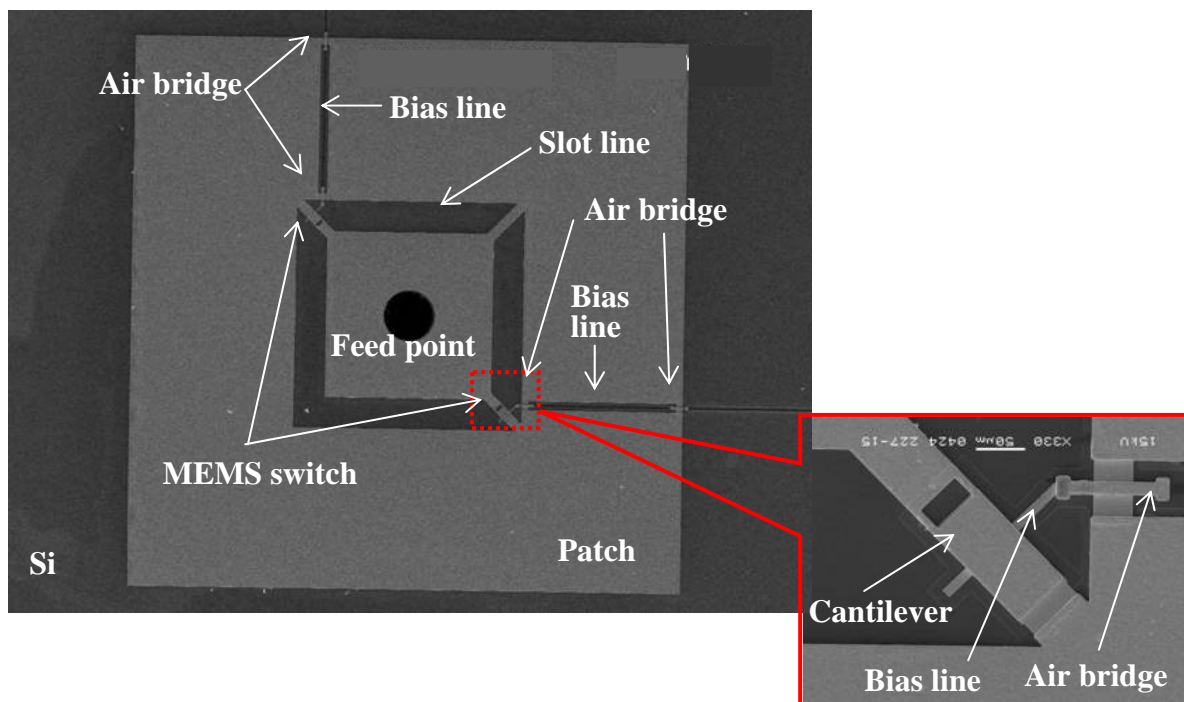


Fig. 2: Prototype of the antenna (SEM)

Table 1: Relation between the width of the conductor and the current density

No. of section	#1	#2	#3	#4	#5
Thickness of conductor ($\times 10^3 \lambda$)	0.02	0.02	0.02	0.19	0.02
Original width of conductor ($\times 10^3 \lambda$)	1.37	2.06	1.37	2.06	2.06
Original current density (A/m)	1.08	0.6	0.55	0.45	0.3
Improved width of conductor ($\times 10^3 \lambda$)	2.75	2.06	2.75	2.06	2.06
Improved current density (A/m)	0.45	0.6	0.55	0.45	0.3

(λ : wavelength at the resonant frequency)

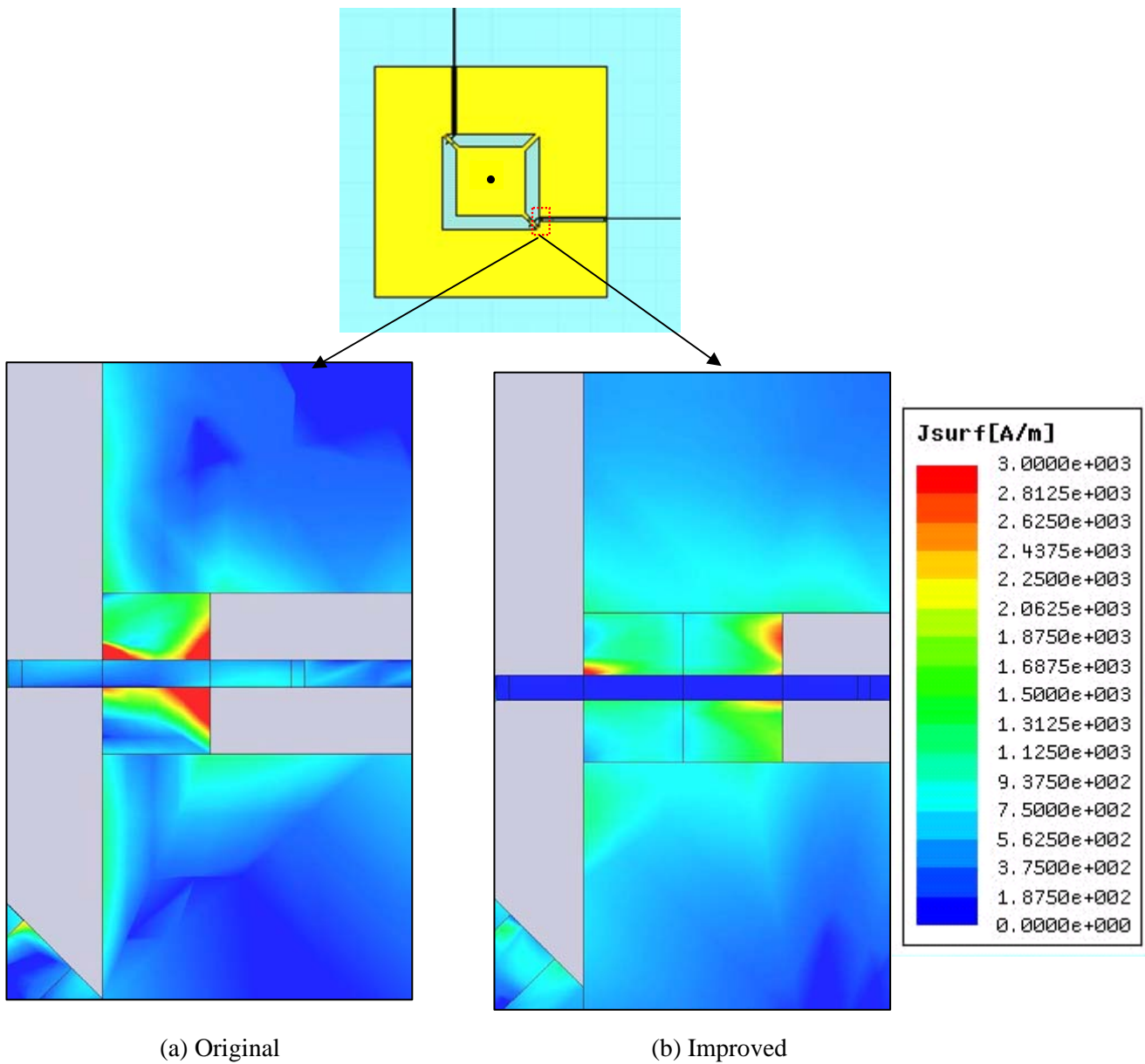


Fig. 3: Current distribution at section #1